Vibrational spectrum of the endohedral Y_{2}C_{2}@C_{92} fullerene by Raman spectroscopy: Evidence for tunneling of the diatomic C_{2} molecule

Brian G. Burke, Jack Chan, Keith A. Williams, Timothy Fuhrer, Wujun Fu, Harry C. Dorn, Alexander A. Puretzky, and David B. Geohegan

Phys. Rev. B **83**, 115457 — Published 29 March 2011

DOI: 10.1103/PhysRevB.83.115457

Vibrational spectrum of the endohedral $Y_2C_2@C_{92}$ fullerene by Raman spectroscopy: Evidence for tunneling of the diatomic C_2 molecule

Brian G. Burke,[1,*] Jack Chan,[1] Keith A. Williams,[1] Timothy Fuhrer,[2] Wujun Fu,[2] Harry C. Dorn,[2] Alexander A. Puretzky,[3] and David B. Geohegan[3]

[1]*Department of Physics, University of Virginia, Charlottesville, Virginia 22904*
[2]*Department of Chemistry, Virginia Polytechnic Institute and State University, Blacksburg, Virginia 24061*
[3]*Materials Science and Technology Division, Center for Nanophase Materials Sciences, Oak Ridge National Laboratory, Oak Ridge, Tennessee 37831*

The structure and vibrational spectrum of the novel endohedral fullerene $Y_2C_2@C_{92}$ was studied by Raman spectroscopy, with particular emphasis on the rotational transitions of the diatomic C_2 unit in the low energy Raman spectrum. We report evidence for tunneling of this unit through the C_2 rotation plane and observe anomalous narrowing in a hindered rotational mode. We also report complementary density functional theory (DFT) calculations that support our conclusions and discuss potential applications to quantum computing and nonvolatile memory devices.

PACS numbers: Valid PACS appear here
Keywords: endohedral fullerenes, metallofullerenes, quantum rotator, raman spectroscopy, yttrium, tunneling

I. INTRODUCTION

Endohedral fullerenes[1] or endofullerenes created by arc-vaporization[2] have been shown to encapsulate clusters of the form M_2C_2 (M = Sc, Y, and several lanthanides)[3]. Within these molecules, entirely novel core species are stable and generate completely new behavior. Recently, these materials have shown promise for numerous applications including electronic devices[4], organic solar cells[5], components for spin-based quantum computing[6,7], and for medical purposes as labels and therapeutic agents[3,8–22]. The fullerene cage (less than 1 nm in diameter) acts to protect the interior complex and can provide ways of maintaining selected properties of the clusters, such as magnetism, fluorescence, and radioactivity, while the endofullerene is functionalized. Endohedral clusters are able to donate additional free electrons to the cage and carrier conduction through encapsulated ions has been observed in endofullerene FETs[4]. Endofullerene LUMO energies are much higher than other organic solar cells, which provide higher open circuit voltages and device efficiencies[5]. Additionally, the electron spin of certain endofullerenes has a remarkably long lifetime, which is useful for qubits in quantum computation[6].

In these materials, the interaction between the endohedral core cluster and the carbon cage gives rise to interesting dynamics that may be studied by Raman and NMR spectroscopy. For example, spectroscopic analyses of $Sc_2C_2@C_{84}$[23] and $Gd_2C_2@C_{92}$[3,24,25] have been reported in the past. Here, we present a detailed Raman spectroscopic analysis of $Y_2C_2@C_{92}$, including temperature dependence. This new molecule is of particular interest to molecular physics and chemistry because of the unique interaction of the carbide with the Y_2 core and cage structure, as well as the unexpected mode narrowing of hindered rotational modes. Furthermore, to the best of our knowledge, this is the first indication of tunneling in this particular molecule and we discuss possible uses of this tunneling in nonvolatile memory devices.

The $Y_2C_2@C_{92}$ molecules were prepared[26], isolated[27], and characterized[28] through NMR spectroscopy in Prof. Dorn's group at Virginia Tech. X-ray diffraction results of $Gd_2C_2@C_{92}$[3] were used to determine the structure of $Y_2C_2@C_{92}$ through DFT calculations. The structure was calculated by hybrid DFT (B3LYP) utilizing the SCF basis set in the Gaussian 03 package[29] and found to be $Y_2C_2@D_3(85)-C_{92}$ with a planar Y_2C_2 unit (Figure 1). The DFT calculations give 1.27 Å and 4.82 Å for the C−C and Y−Y distances, respectively. Knowledge of the bond length of the carbide allows one to calculate the moment of inertia and subsequently the rotational constant B.

II. EXPERIMENT AND RESULTS

Raman microspectroscopy is a powerful technique to study endohedral fullerenes, due to its sensitivity to core−cage interactions and ability to analyze picogram samples. For Raman studies, 10 μg of $Y_2C_2@C_{92}$ were suspended in carbon disulfide (CS_2, 99.999%, Sigma-Aldrich) and used to dropcoat a gold-covered silicon substrate. The resulting polycrystalline films were dried under ambient conditions and placed in an Oxford (MICROHR2) liquid helium optical cryostat. Raman spectra were studied with 632.8 nm excitation from a HeNe laser. The scattered light was collected in the backscattering geometry by a triple-axis spectrometer (Jobin Yvon Horiba, T64000) equipped with a liquid

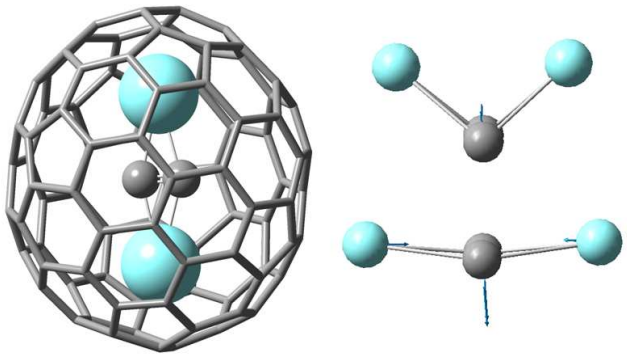

FIG. 1: [color online] (Left) Structure of $Y_2C_2@D_3(85)-C_{92}$ with planar Y_2C_2 unit calculated by DFT. (Right) Simulated DFT butterfly mode, where the two yttrium atoms move in a flapping motion around the carbide base.

nitrogen cooled CCD detector. A resolution of 0.7 cm^{-1} (1800 gr/mm) was used for all Raman measurements and all measurements used 2.5 mW/cm^2 laser power and 30 min. accumulation time. Measurements were performed at selected temperatures from 4.2 K to 300 K.

The Raman spectra observed for $Y_2C_2@C_{92}$ can be separated into three regions: C_{92} cage modes, Y_2C_2-cage modes, and low energy rotational modes, attributed to a free non-rigid C_2 rotor. Figure 2 shows the Raman spectra of $Y_2C_2@C_{92}$ at selected temperatures. Radial C_{92} modes exist above 195 cm^{-1} and the $H_g(1)$ squashing mode is identified at 200.0 cm^{-1}. Below 195 cm^{-1}, two peaks are observed at 163.6 and 182.6 cm^{-1} indicating a hindered rotation due to the interaction of Y_2C_2 to the C_{92} cage. From DFT calculations, the prominent peak at 163.6 cm^{-1} is identified as a *butterfly* mode (Figure 1), since the two yttrium atoms move in a flapping motion around the carbide base. The Y_2C_2 butterfly mode interacts with the C_{92} cage differently than other Y_2C_2 modes. As the temperature decreases below 200 K, the mode becomes narrower, the linewidth decreases. This implies that a C_{92} cage freezing transition has occurred, which then strengthens the interactions between the core complex and the cage. Additionally, the butterfly mode has an observable temperature dependence compared to the C_{92} cage modes which remain roughly unchanged. Other groups have seen evidence for the formation of a M_2C_2-cage interaction[23,24], which reduces the cage symmetry, and have observed mode narrowing, indicated by an increase in intensity and a decrease in linewidth (FWHM).

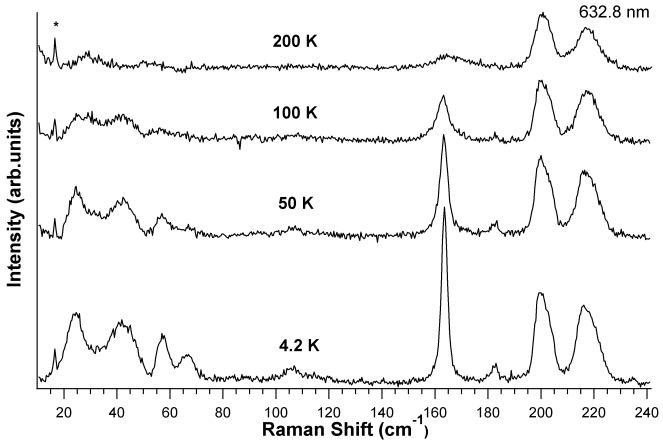

FIG. 2: Low energy Raman spectra of $Y_2C_2@C_{92}$ taken at selected temperatures indicating radial C_{92} modes, hindered rotational modes due to the coupling of the core complex to the cage, and rotational modes of a free non-rigid C_2 rotor (asterisk indicates a plasma line).

Several rotational transitions become apparent as the temperature is decreased and other hindered modes become more intense and the linewidths narrow. In particular, the butterfly mode at 163.6 cm^{-1} undergoes anomalous mode narrowing compared to the relevant C_{92} modes and rotational modes, whose linewidth (FWHM) and intensity remains relatively constant as the temperature decreases. The temperature dependence of the butterfly mode follows an empirical and phenomenological power law that can be modeled by

$$\Gamma = \Gamma_0 + AT^{\gamma}, \tag{1}$$

where $\Gamma_0 = 1.36 \pm 0.04$ cm^{-1}, $A = 9.94 \times 10^{-6} \pm 3.26 \times 10^{-6}$ (cm·K)$^{-1}$, and $\gamma = 2.58 \pm 0.03$. The widths of the butterfly mode as well as two other modes, the $H_g(1)$ cage mode and the lowest C_2 rotational mode, are plotted as a function of temperature in Figure 3. The anomalous mode narrowing we observe for the butterfly mode is reminiscent of the Dicke effect or collisional narrowing[30,31], which has been observed in other systems such as Rb^{87} atoms in spherical storage cells[32] and O_2 in nanoporous Al_2O_3[33]. Our data suggests that at high temperatures, the linewidth is controlled by thermal Doppler broadening and intermolecular collisions[33], whereas the narrowing mechanism may control the linewidth at lower temperatures.

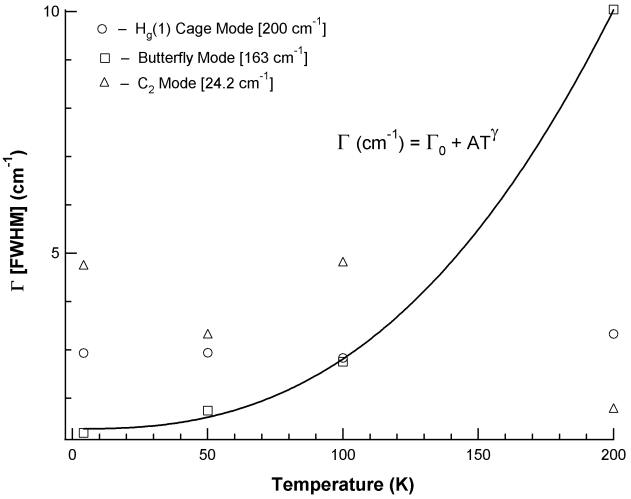

FIG. 3: The width (FWHM) of three Raman modes plotted against temperature. The butterfly mode (163.6 cm^{-1}) undergoes a mode narrowing as the temperature decreases and can be modeled by a power law. Other modes show no significant change in width or intensity as the temperature is lowered.

Low energy quantized rotational states of a free non-rigid C_2 rotor are identified from 24−107 cm^{-1}. Similar spectra have been observed in Sc_2C_2@C_{84} for a C_2 plane rotor, as well as a C−C stretch vibration at 1745 cm^{-1}[23]. For a free non-rigid C_2 rotor, the energy eigenvalues are given by

$$E(J) = BJ(J+1) - DJ^2(J+1)^2, \tag{2}$$

where $B(\text{cm}^{-1}) = \frac{27.9865\times10^{-47}}{I_C(kg\cdot m^2)}$ is the rotational constant, $I_C = \frac{1}{2}m_C R_C^2$ is the moment of inertia, and $D = \frac{4B^3}{\omega^2}$[34]. The value of $R_C = 1.27$ Å determined by our DFT calculations gives a value of $B = 1.73$ cm^{-1}. The factor D accounts for the centrifugal force, but since the vibrational frequency $\omega = 1745$ cm^{-1} is so high, we may disregard the second term of $E(J)$.

As the temperature is lowered from room temperature, rotational peaks appear and become less broadened. In Figure 4, the experimental data (open circles) at 4.2 K have been fitted using Lorentzian functions and the values are listed in Table I. These values correspond to the even rotational states of a freely rotating C_2 molecule and follow the Raman selection rule $\Delta J = \pm 2$[34]. A comparison of these values is shown in Table I.

TABLE I: Comparison of experimental low energy Raman peaks with the calculated rotational states of a freely rotating C_2 molecule. Raman transitions are shown in parentheses. The experimental values were determined from the 4.2 K data set. Calculated values were determined from $B = 1.73$ cm^{-1} and $\Delta J = \pm 2$.

Experiment (cm^{-1})	Free C_2 rotor (cm^{-1})
24.2	24.2 (2 → 4)
42.2	38.1 (4 → 6)
57.0	51.9 (6 → 8)
66.9	65.7 (8 → 10)
106.1	107.3 (14 → 16)

An unperturbed rotational state can only be observed if the rotational barriers are ≈ 0 eV. Due to the charge coupling interaction between the carbide and yttrium atoms, an effective potential barrier must be considered. Additionally, there appears to be a repulsive cage contribution due to charge coupling interactions near 6−6−5 intersections (Figure

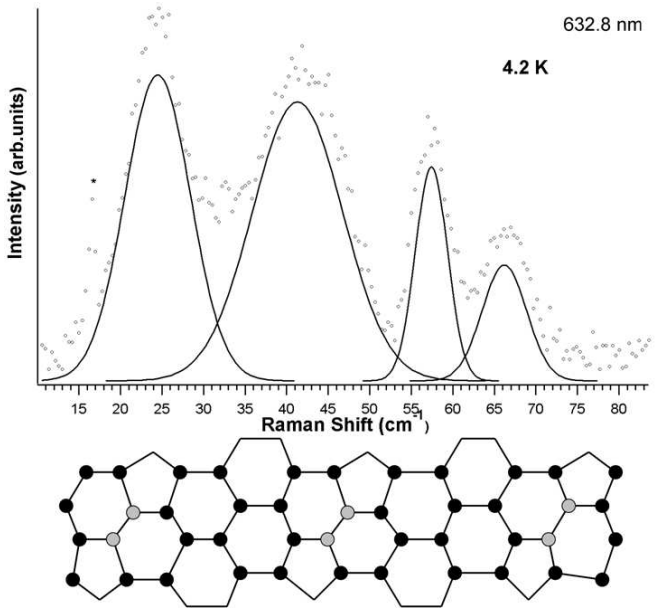

FIG. 4: [color online] (Top) Analysis of low energy Raman rotational lines of $Y_2C_2@C_{92}$ taken at 4.2 K indicating the even rotational levels of a free non-rigid C_2 rotor (asterisk indicates a plasma line). (Bottom) Motif of 6−6−5 cage intersections (identified in grey), which provide a repulsive rotational barrier to the Y_2C_2 complex.

4). From DFT calculations, we observe an average rotational barrier of $V_0 = 107.7$ meV after every 120° of rotation around the C_2 rotation plane (Figure 5). Therefore, we can denote this rotational barrier as $V(\theta) = V_0\cos^2(1.5\theta)$. This energy barrier explains the slight deviation of the peak Raman values from the theoretical free C_2 rotor.

A combination of Raman and recent NMR spectral data[28], which identifies a triplet state (1:2:1) for C_2, and DFT calculations explains the complex rotational and vibrational motion of the Y_2C_2 cluster in the $Y_2C_2@C_{92}$ molecule. As indicated in Figure 5, the cluster undergoes a rotation that can be described as a *carousel*: the yttrium atoms are analogous to the axis of the carousel and the carbons of the carbide rotate around the axis. As one carbon of the C_2 unit moves up, the other moves down while rotating around the Y_2 axis in the C_2 rotation plane. This motion suggests the tunneling of the C_2 unit through the C_2 rotation plane. The Y_2 axis and C_2 axis are defined as the axis connecting the homopolar (A_2, A = Y, C) molecule which is coincident with the chemical bond.

The C_2 unit tunnels through three states perpendicular to the Y_2 axis (-60°, 0°, and 60°) at energy differences 0 meV, 79.3 meV, and 0 meV, respectively. There is a large amount of charge coupling between the core complex and the cage and any additional voltage applied to the cage will redistribute the charge isotropically. The electronic distribution of the endofullerene $Y_2C_2@C_{92}$ may be approximated by the ionic model, $(Y_2C_2)^{4+}@C_{92}^{4-}$. In this model, the yttrium ions exist in their usual Y^{3+} state, while the C_2 unit is considered an acetylide ion, C_2^{2-}, and the core complex transfers four electrons to the carbon cage to stabilize the molecule. An applied voltage to the cage, greater than the energy differences of the three C_2 orientations in the "0" state, would negate the Y_2C_2 interactions with the 6−6−5 cage intersections. The C_2 unit would cease to tunnel through the C_2 rotation plane, since the core complex would experience an isotropic rotation barrier instead of $V(\theta)$.

By applying a small voltage (100 meV) to the cage, which should distribute isotropically and provide additional charge to the core, the C_2 unit would be excited into the "1" state, being completely perpendicular to the Y_2 axis. When the voltage is removed, the carbide would return to the "0" state and all three orientations would be accessible. This tunneling scheme could provide a single molecule memory device. The molecules can be arranged in arrays by functionalizing the cages and external voltages can be supplied by lithographically defining contacts or utilizing CNT wires[35,36]. Additionally, through nondestructive optical techniques, such as Raman or IR, when the external voltage is applied, there should exist an observable shift in the rotational C_2 modes. Specifically, in the "1" state, the Raman transition $4 \rightarrow 6$ should shift by 4.1 cm^{-1} to 38.1 cm^{-1} and the $6 \rightarrow 8$ transition should shift by 5.1 cm^{-1} to 51.9 cm^{-1}.

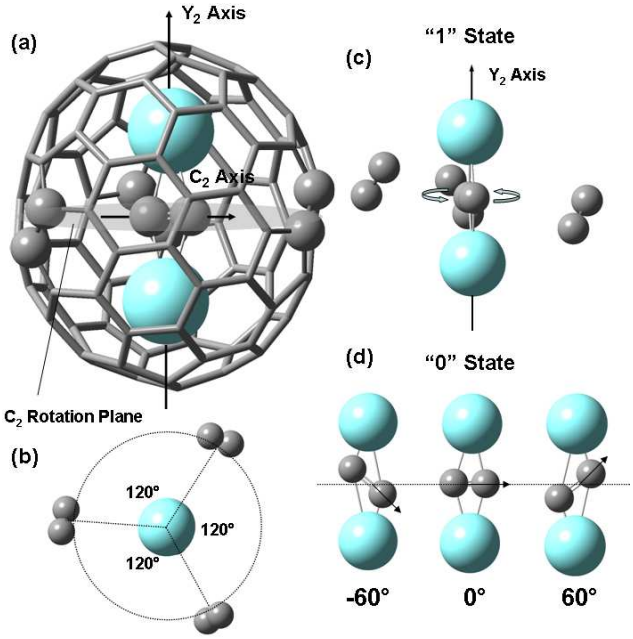

FIG. 5: [color online] (a) $Y_2C_2@D_3(85)-C_{92}$ with planar Y_2C_2 unit and 6−6−5 cage intersections indentified as grey spheres of the cage. The C_2 axis is parallel to the C_2 rotation plane (defined by the 6−6−5 cage intersections) and perpendicular to the Y_2 axis, which is orthogonal to the C_2 rotation plane. The Y_2 axis and C_2 axis are defined as the axis connecting the homopolar (A_2, A = Y, C) molecule which is coincident with the chemical bond. (b) Top view of the C_2 rotation plane, which indicates a repulsive interaction between the C_2 rotor and the 6−6−5 cage intersections after every 120° of rotation about the Y_2 axis. (c) "1" state; all C_2 rotations about the Y_2 axis remain parallel to the C_2 rotation plane due to an applied voltage (100 meV) which removes the effect of the rotational barrier $V(\theta)$. (d) "0" state; C_2 rotations about the Y_2 axis alternate between three states, -60°, 0°, and 60°, which tunnel through the C_2 rotation plane due to the rotational barrier $V(\theta)$.

III. CONCLUSIONS

We have described the structure and vibrational spectrum of $Y_2C_2@C_{92}$. The molecule was characterized by Raman spectroscopy and DFT molecular modeling. Radial cage modes, low energy Y_2C_2−cage modes, and rotational transitions of a diatomic C_2 unit were identified in the Raman spectra. We observed anomalous mode narrowing and a temperature dependence for a Y_2C_2 hindered rotational mode, identified as a butterfly mode. Experimental Raman peaks are slightly deviated from the theoretical free diatomic rotor values, which signifies a rotational barrier and tunneling of the C_2 unit. A triplet (1:2:1) in recent NMR data[28] observed for C_2 further suggests the tunneling of the C_2 unit through the C_2 rotational plane. From DFT calculations, this tunneling is attributed to a rotational barrier, $V(\theta) = V_0\cos^2(1.5\theta)$, caused by charge coupling interactions near 6−6−5 cage intersections. The rotational and vibrational motion of the Y_2C_2 cluster in the $Y_2C_2@C_{92}$ molecule functions as a carousel. To the best of our knowledge, this system is the first experimental observation of a freely rotating non-rigid C_2 diatomic rotor in endohedral fullerenes and the first to indicate tunneling of the C_2 unit.

IV. ACKNOWLEDGEMENTS

We are grateful for support of this work by the National Science Foundation [CHE-0443850 (H.C.D.), DMR-0507083 (H.C.D.)] and the National Institutes of Health [1R01-CA119371-01 (H.C.D.)]. A portion of this research at Oak Ridge National Laboratory's Center for Nanophase Materials Science was sponsored by the Scientific User Facilities Division, Office of Basic Energy Sciences, U.S. Department of Energy.

* Corresponding Author: bgb9q@virginia.edu

[1] J. Heath, S. C. O'Brien, Q. Zhang, Y. Liu, R. F. Curl, F. K. Tittel, and R. E. Smalley, J. Am. Chem. Soc. **107**, 7779 (1985).

[2] S. Stevenson, G. Rice, T. Glass, K. Harich, F. Cromer, M. R. Jordan, J. Craft, E. Hajdu, R. Bible, M. M. Olmstead, K. Maitra, A. J. Fisher, A. L. Balch, and H. C. Dorn, Nature **401**, 55 (1999).
[3] H. Yang, C. Lu, Z. Liu, H. Jin, Y. Che, M. M. Olmstead, and A. L. Balch, J. Am. Chem. Soc. **130**, 17296 (2008).
[4] S. Kobayashi, S. Mori, S. Iida, H. Ando, T. Takenobu, Y. Taguchi, A. Fujiwara, A. Taninaka, H. Shinohara, and Y. Iwasa, J. Am. Chem. Soc. **125**, 8116 (2003).
[5] R. B. Ross, C. M. Cardona, D. M. Guldi, S. G. Sankaranarayanan, M. O. Reese, N. Kipipdakis, J. Peet, B. Walker, G. C. Bazan, E. Van Keuren, B. C. Holloway, and M. Drees, Nature Materials **8**, 208 (2009).
[6] W. Harneit, Phys. Rev. A **65**, 032322 (2002).
[7] J. A. Larsson, J. C. Greer, W. Harneit, and A. Weidinger, J. Chem. Phys. **116**, 7849 (2002).
[8] H. Kato, Y. Kanazawa, M. Okumura, A. Taninaka, T. Yokawa, and H. Shinohara, J. Am. Chem. Soc. **125**, 4391 (2003).
[9] T. Zuo, L. Xu, C. M. Beavers, M. M. Olmstead, W. Fu, T. D. Crawford, A. L. Balch, and H. C. Dorn, J. Am. Chem. Soc. **130**, 12992 (2008).
[10] S. R. Zhang, D. Y. Sun, X. Y. Li, F. K. Pei, and S. Y. Liu, Fullerene Sci. Technol. **5**, 1635 (1997).
[11] L. J. Wilson, D. W. Cagle, T. P. Thrash, S. J. Kennel, S. Mirzadeh, J. M. Alford, and G. J. Ehrhardt, Coord. Chem. Rev. **192**, 199 (1999).
[12] L. J. Wilson, *The Electrochemical Society Interface*, Winter, 24 (1999).
[13] M. Mikawa, H. Kato, M. Okumura, M. Narataki, Y. Kanazawa, N. Miwa, and H. Shinohara, Bioconjugate Chem. **12**, 510 (2001).
[14] E. B. Iezzi, J. C. Duchamp, K. R. Fletcher, T. E. Glass, and H. C. Dorn, Nano Lett. **2**, 1187 (2002).
[15] M. Okumura, M. Mikawa, T. Yokawa, Y. Kanazawa, H. Kato, and H. Shinohara, Academic Radiology **9**, S495 (2002).
[16] R. D. Bolskar, A. F. Benedetto, L. O. Husebo, R. E. Price, E. F. Jackson, S. Wallace, L. J. Wilson, and J. M. Alford, J. Am. Chem. Soc. **125**, 5471 (2003).
[17] P. P. Fatouros, F. D. Corwin, Z. J. Chen, W. C. Broaddus, J. L. Tatum, B. Kettenmann, Z. Ge, H. W. Gibson, J. L. Russ, A. P. Leonard, J. C. Duchamp, and H. C. Dorn, Radiology **240**, 756 (2006).
[18] E. Zhang, C. Shu, L. Feng, and C. Wang, J. Phys. Chem. B **111**, 14223 (2007).
[19] B. Sitharaman and L. J. Wilson, J. Biomed. Nanotechnol. **3**, 342 (2007).
[20] M. N. Chaur, F. Melin, A. J. Athans, B. Elliott, K. Walker, B. C. Holloway, and L. Echegoyen, Chem. Commun. **23**, 2665 (2008).
[21] C. Shu, C. Wang, J. Zhang, H. W. Gibson, H. C. Dorn, F. D. Corwin, P. P. Fatouros, and T. J. S. Dennis, Chem. Mater. **20**, 2106 (2008).
[22] C. Shu, X. Ma, J. Zhang, F. D. Corwin, J. H. Sim, E. Y. Zhang, H. C. Dorn, H. W. Gibson, P. P. Fatouros, C. R. Wang, and X. H. Fang, Bioconjugate Chem. **19**, 651 (2008).
[23] M. Krause, M. Hulman, H. Kuzmany, O. Dubay, G. Kresse, K. Vietze, G. Seifert, C. Wang, and H. Shinohara, Phys. Rev. Lett. **93**, 137403 (2004).
[24] B. G. Burke, J. Chan, K. A. Williams, J. Ge, C. Shu, W. Fu, H. C. Dorn, A. A. Puretzky, and D. B. Geohegan, Mater. Res. Soc. Symp. **1204**, K10 (2009).
[25] B. G. Burke, J. Chan, K. A. Williams, J. Ge, C. Shu, W. Fu, H. C. Dorn, J. G. Kushmerick, A. A. Puretzky, and D. B. Geohegan, Phys. Rev. B **81**, 115423 (2010).
[26] W. Fu, L. Xu, H. Azurmendi, J. Ge, T. Fuhrer, T. Zuo, J. Reid, C. Shu, K. Harich, and H. C. Dorn, J. Am. Chem. Soc. **131**, 11762 (2009).
[27] Z. Ge, J. C. Duchamp, T. Cai, H. W. Gibson, and H. C. Dorn, J. Am. Chem. Soc. **127**, 16292 (2005).
[28] T. Fuhrer, W. Fu, H. C. Dorn, B. G. Burke, and K. A. Williams, J. Am. Chem. Soc. (in publication).
[29] M. J. Frisch *et al.*, *Gaussian 03*, Revision C.02, Gaussian Inc.: Willingford, CT (2004).
[30] R. H. Dicke, Phys. Rev. **89**, 472 (1953).
[31] R. P. Frueholz and C. H. Volk, J. Phys. B: At. Mol. Phys. **18**, 4055 (1985).
[32] R. P. Frueholz and J. C. Camparo, Phys. Rev. A **35**, 3768 (1987).
[33] T. Svensson and Z. Shen, Appl. Phys. Lett. **96**, 021107 (2010).
[34] G. Herzberg, *Molecular Spectra and Molecular Structure: I. Spectra of Diatomic Molecules* (D. Van Nostrand Company, New York, 1939).
[35] Y. K. Kwon, D. Tomanek, and S. Iijima, Phys. Rev. Lett. **82**, 1470 (1999).
[36] Y. Yasutake, Z. Shi, T. Okazaki, H. Shinohara, and Y. Majima, Nano Lett. **5**, 1057 (2005).